

AD-A250 991

ATION PAGE

Form Approved
OMB No. 0704-0188

to average 1 hour per response, including the time for reviewing instructions, searching existing data sources, gathering the collection of information. Send comments regarding this burden estimate or any other aspect of this form, to Washington Headquarters Services, Directorate for Information Operations and Reports, 1215 Jefferson Avenue, Washington, DC 20540.

DATE

05-15-92

3. REPORT TYPE AND DATES COVERED

Technical

06-01-91 to 05-31-92

4. TITLE AND SUBTITLE

The Chemistry and Packaging of Nanocomposite
Confined Arrays

5. FUNDING NUMBERS

N00014-90-J-1159

6. AUTHOR(S)

G.D. Stucky

7. PERFORMING ORGANIZATION NAME(S) AND ADDRESS(ES)

University of California
Department of Chemistry
Santa Barbara, CA 93106

8. PERFORMING ORGANIZATION
REPORT NUMBER

T20

9. SPONSORING/MONITORING AGENCY NAME(S) AND ADDRESS(ES)

Office of Naval Research
Chemistry Program
800 N. Quincy Street
Alexandria, VA 22217

10. SPONSORING/MONITORING
AGENCY REPORT NUMBER

11. SUPPLEMENTARY NOTES

Prepared for Publication in Materials Research Society Symposium
Proceedings, Volume 206

12a. DISTRIBUTION/AVAILABILITY STATEMENT

Approved for public release;
distribution unlimited

12b. DISTRIBUTION CODE

13. ABSTRACT (Maximum 200 words)

The miniaturization of electronic and optic devices has revolutionized response times, energy loss and transport efficiency. An additional bonus is that as one approaches the nanosize regime the presence or absence of a few atoms and the geometrical disposition of each atom can significantly modify electronic and photonic properties. This control can be further supplemented by "packaging" assemblies of atoms or molecules into thin film or nanocomposite bulk materials to define surface states, cluster environment and geometry, intercluster interactions, and consequently, a wide tunable range of optical and charge carrier responses.

The chemist is presented with an intriguing challenge. First the clusters must be unisized with identical geometries. Secondly, the atom or molecular assemblies should ideally have perfect periodicity in order to rigorously define optoelectronic densities and intercluster tunnelling. A third requirement is that the nanocomposite be processable, generally in the form of thin films or single crystals. Numerous approaches are being undertaken in achieving these goals, including molecular beam and atomic layer epitaxy, molecular sieve inclusion chemistry, molecular capping of inorganic clusters, porous glass and aerosol synthesis. This paper presents a brief review of the interface chemistry associated with nanophase confinement and packaging and some features of three dimensional surface confinement using molecular sieves and zeolites.

14. SUBJECT TERMS

15. NUMBER OF PAGES

16

16. PRICE CODE

17. SECURITY CLASSIFICATION
OF REPORT

Unclassified

18. SECURITY CLASSIFICATION
OF THIS PAGE

Unclassified

19. SECURITY CLASSIFICATION
OF ABSTRACT

Unclassified

20. LIMITATION OF ABSTRACT

UL

OFFICE OF NAVAL RESEARCH

**Contract N00014-90-J-1159
R&T Code 413n007**

Technical Report No. 20

**The Chemistry and Packaging of
Nanocomposite Confined Arrays**

**by
G.D. Stucky**

Prepared for Publication in

**Materials Research Society
Symposium Proceedings
Volume 206**

May 15, 1992

Reproduction in whole or in part is permitted for any purpose of the United State Government.

This document has been approved for public release and sale; its distribution is unlimited.

This statement should also appear in Item 12 of the Report Documentation Page, Standard Form 298. Your contract number and R&T Code should be reported in Item 5 of Standard Form 298. Copies of the form are available from your cognizant grant or contract administrator.

THE CHEMISTRY AND PACKAGING OF NANOCOMPOSITE CONFINED ARRAYS

GALEN D. STUCKY

Department of Chemistry, University of California, Santa Barbara, CA 93106

ABSTRACT

The miniaturization of electronic and optic devices has revolutionized response times, energy loss and transport efficiency. An additional bonus is that as one approaches the nanosize regime the presence or absence of a few atoms and the geometrical disposition of each atom can significantly modify electronic and photonic properties. This control can be further supplemented by "packaging" assemblies of atoms or molecules into thin film or nanocomposite bulk materials to define surface states, cluster environment and geometry, intercluster interactions, and consequently, a wide tunable range of optical and charge carrier responses.

The chemist is presented with an intriguing challenge. First the clusters must be unified with identical geometries. Secondly, the atom or molecular assemblies should ideally have perfect periodicity in order to rigorously define optoelectronic densities and intercluster tunnelling. A third requirement is that the nanocomposite be processable, generally in the form of thin films or single crystals. Numerous approaches are being undertaken to achieve these goals, including molecular beam and atomic layer epitaxy, molecular sieve inclusion chemistry, molecular capping of inorganic clusters, porous glass and aerosol synthesis. This paper presents a brief review of the interface chemistry associated with nanophase confinement and packaging and some features of three dimensional surface confinement using molecular sieves and zeolites.

Introduction

Because of the importance of nanocluster chemistry to a wide variety of fields ranging from atom and electron transport in biological systems, heterogeneous catalysis, photo-catalysis, to the development of new electro-optic devices based on quantum confinement, there has been an explosion of interest in this area by scientists from many areas. Syntheses of nanoclusters have been carried out in numerous ways to give unexpectedly different materials with varied structural, optical, and transport properties. Molecular inorganic, physical and biochemists have generated nanoclusters by building up arrays from solution or gas phases atom by atom [1,2,3]. From the other directions, solid state physicists and engineers have focused on increasingly smaller and smaller dimensions with engineering based directly on a solid state atomic lattice substrates [4,5]. The materials chemistry at this molecular and solid state interface requires a precise definition of the number of atoms, their siting (e.g. bulk versus surface), and ultimately the manner in which they are assembled to form a nanocomposite array. It is for these reasons that while the convergence of molecular and solid state chemistry is near, the somewhat diffuse materials synthesis interface between isolated clusters and the infinite solid array is only beginning to be resolved.

Current Nanocluster Synthetic Methodologies

Chemists have pushed metal atom clusters to their limits over the past 30 years so that there is the most detailed information about their synthesis and detailed structures. The largest metal-metal bonded nanocluster which has been synthesized and structurally characterized by single crystal diffraction measurements is $[\text{Hf}_{138}\text{Pt}_6(\text{CO})_{48}]^{5-}$ [6]. In this regime the structures (Figure 1) can be thought of as small chunks of metal which are solubilized by a coating of ligands. Studies of metal nanoclusters beautifully demonstrate the fact that the bonding at the exterior surface of the nanocluster can energetically dominate the ultimate cluster geometry. For example, the dimensions of these fragments are large enough so that one observes the hexagonal and cubic close packed arrangement of metal atoms in $[\text{Pt}_{26}(\text{CO})_{32}]^{2-}$ and $[\text{Pt}_{38}(\text{CO})_{44}\text{H}_2]^{2-}$ clusters respectively [7]. However, in $[\text{Pt}_{15}(\text{CO})_{30}]^{2-}$, the platinum metal atoms arrange themselves in a helical array of triangular Pt_3 units and in $[\text{Pt}_{19}(\text{CO})_{30}]^{2-}$ the metal cluster is a bicapped pentagonal-prism similar to the geometry reported for certain microcrystalline materials such as metal dendrites and whiskers [8]. These geometries are still an unresolved challenge to theoretical chemistry as well as to the development of useful predictive theories for nucleation phenomena.

The ultimate limit of how far the solution chemist can go in nanocluster synthesis remains to be

92-14130



92 5 28 068

determined. The above clusters are in fact relatively small, the largest being 7 platinum atoms in the longest

Convergence of Molecular and Solid State Chemistry

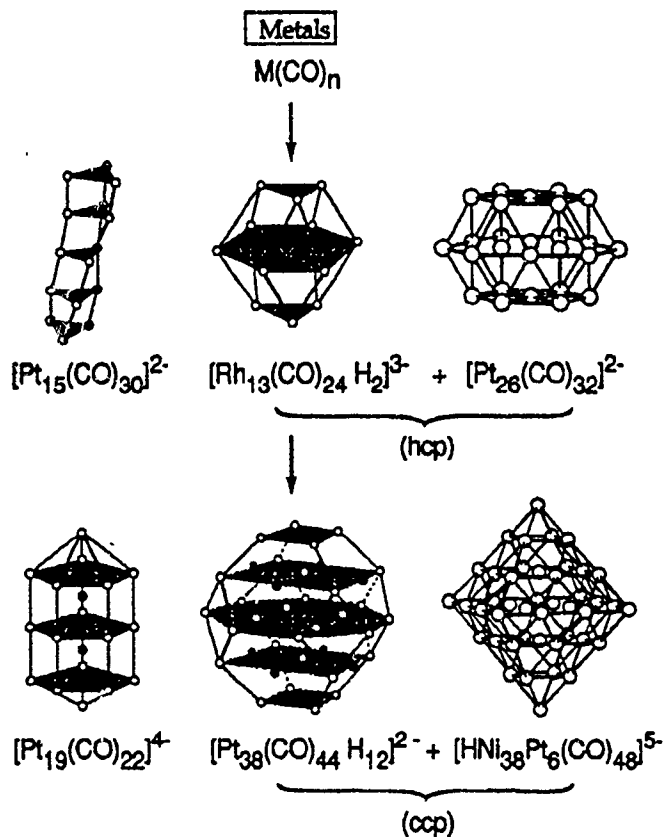


Figure 1: Structurally characterized metal atom clusters

dimension ($\sim 16 \text{ \AA}$). Schmid has reported a family of clusters based on the closest packing of atoms to give "magic" numbers of 13, 55, etc. with the n th shell containing $10n^2 + 2$ atoms. Examples include $\text{Au}_{55}(\text{P}(\text{Ph})_2)_{126}^{6+}$ ($\text{Ph} = \text{C}_6\text{H}_5$) and $\text{Pd}_{561}(\text{phen})_{36}\text{O}_{190-120}$ ($\sim 26 \text{ \AA}$ in diameter with 5 spherical shells, and phen = phenanthroline)^[9]. Isolation and characterization of a pure phase of the latter has not yet been reported.

Using solution phase reactions, Dance has created soluble molecular clusters such as $[\text{C}_{10}\text{S}_4(\text{SPh})_{16}]^{4-}$ (Fig. 2) which can be considered as fragments of the bulk semiconductor lattice^[10,11,12]. As molecular entities these can be isolated and structurally characterized with the largest structurally characterized cluster reported to date being $[\text{Cd}_{17}\text{S}_4(\text{SPh})_{28}]^{2-}$ ^[13]. This structure forms tetrahedrally coordinated Cd and S atoms as does bulk CdS, however each Cd atom is also bonded to a surface S atom which is part of the thiophenol group. This manner of covalent bonding at the surface forms a method for control of cluster aggregation and

gives a monodisperse size. Notice that the ratio of Cd:S in this material is not 1:1 but 1:2. This

Convergence of Molecular and Solid State Chemistry

Semiconductors

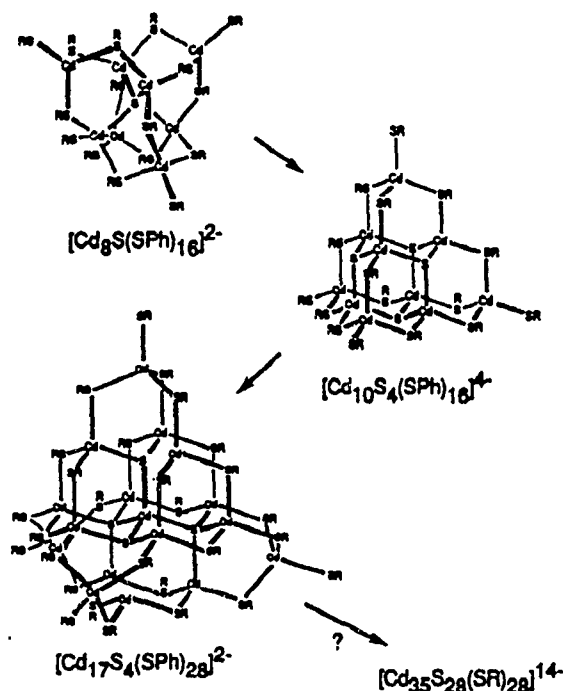


Figure 2. Structurally characterized II-VI clusters. M= Zn,Cd; E=S,Se,Te; R=C₆H₅ [18],[19],[20]

nonstoichiometry is common among small particle semiconductors as will be discussed for GaP included in zeolites in the next section. As illustrated in Figure 2, one again finds the possibilities of a variety of nanocluster geometries. Cheng, Herron and Wang^[14] demonstrated that even very small clusters such as these have large nonresonant nonlinearities; the Dance compound has a nonresonant nonlinearity comparable to that of conjugated organic dye molecules and bigger clusters have even larger nonlinearities.

The initial work in the area of larger small particle semiconductors (10 ~ 100 Å) described by Brus and Steigerwald^[15,16] deals with the formation of size quantized particles in colloidal solution, their characterization, and interpretation of this data using both classical molecular orbital theory and some quantum mechanics. The chemistry needed to generate nanoclusters is indeed state-of-the-art requiring control of kinetic parameters beyond the limits of that which have been previously achieved in solution chemistry^[17]. The goal is essentially to arrest a runaway reaction which given sufficient starting materials will result in the generation of a bulk material. The appropriate cluster size is achieved by competitive reaction chemistry between core cluster growth and surface capping which terminates the cluster growth. Kinetic control of the

Accession For		
NTIS	CRA&I	<input checked="" type="checkbox"/>
DTIC	TAB	<input type="checkbox"/>
Unannounced		<input type="checkbox"/>
Justification		
By		
Distribution		
Advanced Development		
Dist	Advanced Development	Special
A-1	20	



average particle size is achieved by adjusting the rate of diffusion, choice of solvent, reaction temperature, reaction time, reagent concentration and the use of microheterogeneous reaction media. Following the example of Dance, strong coordinating ligands are then used to abruptly terminate cluster growth^[18,19,20]. Analogous to the ferritin example described below, stabilization can be achieved with an inorganic phosphate polymer, such as sodium hexametaphosphate^[21]. The kinetics of the nucleation and passivation processes are fast and in general a typical preparation gives a poly dispersity of $\pm 10\%$ in particle diameter^[11,2]. Control of cluster size, stability of clusters toward aggregation, and differentiation of cluster-cluster interactions from surface or other effects are drawbacks to colloidal methods.

Theopold and coworkers^[22] have devised a synthesis to give small particle III-V semiconductors through what is essentially the hydrolysis of a monomeric arsinogallane. The reaction of $(C_5(CH_3)_5)GaAs(Si(CH_3)_3)_2$ with 2 equivalents of *t*-butanol, shown in Figure 3, yields over several hours small GaAs particles as evidenced by the shift to longer wavelength in the UV-Vis spectrum

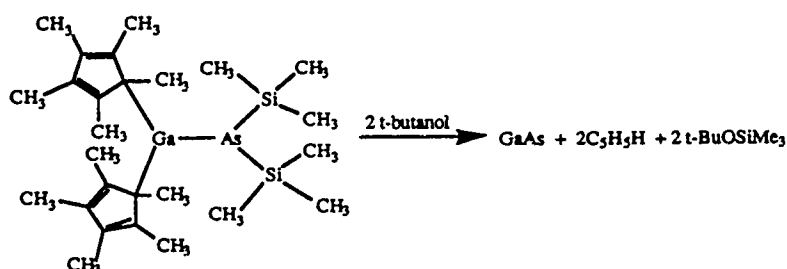


Figure 3. Reaction of $(C_5(CH_3)_5)GaAs(Si(CH_3)_3)_2$ with *t*-butanol to form GaAs.

with time. This is the first example of a solution phase reaction which yields size quantized III-V semiconductors. This reaction is not controlled as in the capped clusters, but goes on to form bulk GaAs through the course of the reaction. More recently Wells and Alivisatos have successfully been able to carry out arrested precipitation reactions to form capped GaAs clusters so that III-V nanoclusters are accessible^[23]. Other methods to prepare size quantized semiconductors include formation of PbS particles on ethylene-methacrylic acid copolymers^[24], and the formation of glass matrices around colloidal solutions of CdS^[25]. In all of these systems, quantum confinement is in three dimensions and the structures are referred to as quantum dots or boxes.

Another intriguing route, also discussed in this symposium, is the creation of nanoclusters by biosynthetic related processes. Nature creates quantum confined clusters of CdS in an elegant way by using short chelating peptides in yeast as part of the biochemical mechanism of entrapping heavy metal atoms such as Cd^[26]. At the time of their characterization, these clusters were found to be more monodisperse than those which had been prepared chemically. Bio- and bioinorganic chemists have studied nanophase cluster formation in a variety of other systems, particularly in the iron transport ferritin^[27,28,29]. Ferritin consists of a shell of proteins derived from nucleotides which surround an iron core of up to 4500 iron atoms that is essentially spherical with a diameter of 80 Å. The composition approximates closely to $(FeOOH)_3(FeO \cdot H_2PO_4)_4$ and the iron core has a close structural resemblance to ferrihydrite, an iron oxide cluster coordinated with water $(5Fe_2O_3 \cdot 9H_2O)$ ^[30] which contains a close packed array of oxide and OH⁻ ions with iron atoms in octahedral interstices. In this case, the phosphate in ferritin serves the role of exterior surface cluster capping and passivation.

The basic science revealed by gas phase studies about cluster stability (e.g. the "magic number" shell model) and surface reactivity are providing valuable guidelines for nanocluster synthesis in condensed phases. Recently, gas phase syntheses of Ga_xAs_y ^[31] and neutral indium phosphide clusters^[32] have been reported. Silicon clusters such as Si^{+}_{45} and gallium arsenide positive cluster ions containing up to 60 atoms have been identified and characterized along with their surface chemistry^[33,34]. In the past there have been no direct structural determinations or means of stabilizing and accumulating the gas clusters so that the use of gas phase precursors for nanocomposite synthesis did not exist. The isolation of C_{60} and C_{70} in large bulk quantities^[35,36] is a major breakthrough that is now generating research activity comparable to that seen previously for high T_c superconducting materials as evidenced by the special session in this symposium.

Nanoclusters and Nanocomposites

In practice the ultimate goal is to construct a multiphase nanocomposite in order to provide photo and thermal stability, form unisized clusters of an arbitrary size, control cluster-cluster interactions, and make device processing available at a high material yield and low cost. In order to design and synthesize the nanocomposite it is necessary to understand the relationship between nanocluster surface chemistry and internal cluster bonding, electronic and structural intercluster coupling, sum and product properties, connectivity patterns, periodicity and scaling, Schottky barrier effects, and coupled phase transformations. Packaging the nanoconfined arrays and controlling these properties is the biggest challenge to the materials scientist.

Undoubtedly the closest overlap between solid state and solution chemistry synthesis of quantum confined nanocomposites has been with 2-d quantum well layered structures. Ishihara and coworkers have recently reported the isolation of a natural quantum well system, $(\text{RNH}_3)_2\text{PbI}_4$ with $\text{R}=\text{C}_{10}\text{H}_{21}$. In this structure, PbI_4^{2-} networks are separated by the alkyl chains of the organic cation RNH_3^+ to give respectively the wells and the potential barriers^[37]. This material has been carefully studied optically and shows marked increase in oscillator strength for the 2D exciton gained by confinement to two dimensions (0.7) compared to that for the 3D exciton in bulk PbI_2 crystal (0.017). The emission spectrum of the exciton in this system is extremely sharp at low temperatures so that the coherence length and perfection of this quantum material appear to be excellent. The consequence is a large third order optical susceptibility, $\chi^{(3)}$, with picosecond or less response time.

Two dimensional surfaces with monolayer or greater thicknesses and combined in various geometrical configurations to give quantum wires or 1-d quantum confinement are currently the basis for optoelectronic devices. The physicist's and engineer's approach to quantum confinement (dots, wires, and layers) has been by way of molecular beam (MBE) and atomic layer epitaxy (ALE)^[38] on an ordered 2-d lattice substrate to fabricate ultra thin (monolayer) semiconductor epitaxial layers. Figure 4 shows how carrier confinement is then achieved by sandwiching the semiconductor layer between two wider-bandgap semiconductor epitaxial layers or by introducing lateral barrier walls to form quantum boxes^[39,40,41]. Quantum wires in which carriers and electronic wave functions have one degree of freedom along an axis can be formed in the MBE approach by corrugation of quantum layers or by lateral structuring^[42,43]. A promising new development is

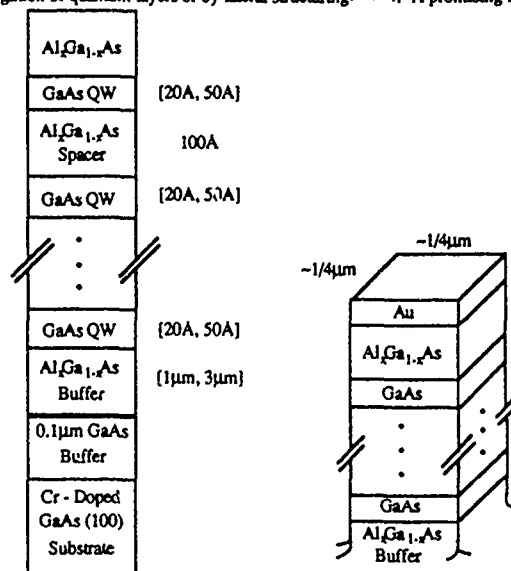


Figure 4. Molecular beam epitaxy derived quantum superlattices.

the use of the scanning tunnel microscope (STM) as a lithographic tool to create barriers on the 10 to 1000 Å

scaled^[44]. Also, epitaxial growth of GaAs on high surface silica has been used to produce size quantized GaAs particles^[45].

For nanoclusters synthesized via solution or gas phase chemistry, the use of capping inorganic and organic groups which have large stability constants is one viable solution. Spin coating of these capped clusters or intrinsic polymerization of functionalized organic caps to give thin film structures then provides a route to device applications. Porous glasses confinement offer less control over the size, shape and cluster-cluster interactions of semiconductor particles within their pores, however, the glasses offer the ease of optical characterization and the potential for use as thin monoliths in optical devices. Another approach is an extension of the solid state approach of using 2-d crystalline surfaces for array organization and definition. By incorporating the confined arrays within a 3-d crystalline surface, i.e. a zeolite or molecular sieve, it is possible to obtain detailed structural information relevant to internal cluster bonding, surface termination, and intercluster coupling. In the following discussion two roles of the 3-d surface are emphasized: 1) the definition of the quantum confinement geometry, and perhaps more importantly, 2) the three dimensional periodicity which directs the formation of a "supra-molecular" composition and the overall quantum lattice^[46,47].

Inclusion and "4th Dimension" Chemistry

Topologically, molecular sieves and zeolites consist of monolayers of edge shared MO_2 tetrahedra. By using large organic and inorganic templates during synthesis these monolayers interconnect into polyhedral or tubular configurations to form cages and channels. This is illustrated in Figure 5 for zeolite RHO ($\text{M}_{12}\text{Al}_{12}\text{Si}_{36}\text{O}_{96}$, M = monovalent cation). Excluding the exterior interconnecting oxygen atoms the cage (point group O_h) is defined by 120 framework Si, Al and O atoms. To graphically simplify the representation, the oxygen atoms between the tetrahedral atom sites are generally omitted as shown in Fig 5b. The sixteen atom ring is then designated by the tetrahedral atoms only as an "eight"

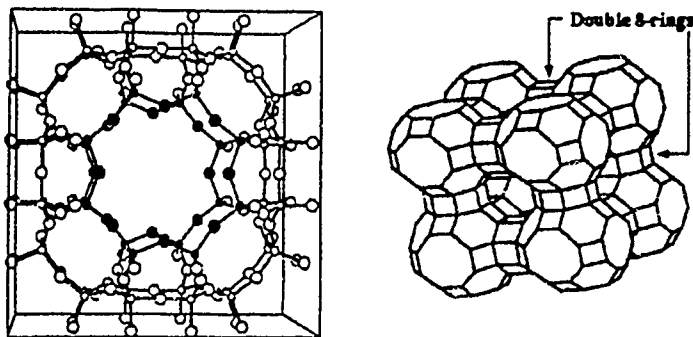


Figure 5. a) Zeolite RHO cage with 120 framework atoms; b) 3-d surface of interconnected cages.

ring. The complete zeolite structure is built up by interconnecting via the six octahedrally located eight rings of the cages. In this zeolite the void space "outside" the cages has exactly the same geometry as that defined by the cages themselves. Every atom in this framework is equally accessible on both sides of the monolayer surface which defines the cage network. It is in every sense a 3-d surface.

As with the nanoclusters described above, it is not clear what the ultimate cage and channel diameters might be. At the present time cages and channels which make up molecular sieves such as zeolite Y^[48] and VPI-5^[49] are known with free diameters of up to 12 Å. The natural mineral caxoxenite possesses 15 Å channels and an 18 Å free diameter channel (Figure 6) has been proposed^[50] so that quantum wires of indefinite length which are one dimensional or form a 2 or 3 dimensional grid network are possible. The

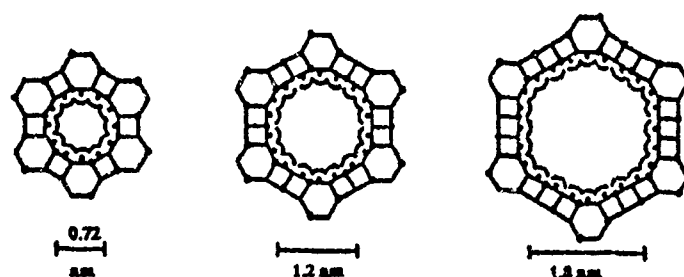


Figure 6. 2-d projections of the first three members of an infinite series of 3-d molecular sieve nets. a) corresponds to AIPO-5 and b) to VPI-5 which was first reported four years after its existence was postulated [50].

quantum confinement is not however determined solely by the cross sectional dimensions of the host channels since the barriers between the quantum dots are one or two insulating atomic layers thick. This means that resonant and indirect tunneling is possible by phonon assisted mechanisms through the overlap of wave functions of adjacent clusters [51,52,53,54].

Table 1
T₄ Corner Shared Molecular Sieve Compositions

	Groups		Charge	
IV-V	SiO ₂	SiO ₂	0	Silicalite
III-V	AlO ₂ ⁻	PO ₂ ⁺	0	AlPO
III-IV-V	AlO ₂ ⁻	(SiO ₂) ₈ (PO ₂ ⁺) ₁₋₈	8	SAPO
III-IV	AlO ₂ ⁻	SiO ₂	1-	Zeolite
IIb-V	ZnO ₂ ²⁻	AsO ₂ ⁺	1-	ZnAsO
II-V	BeO ₂ ¹⁻	PO ₂ ⁺	1-	BEPO
III-III	BO ₂ ⁻	VO ₂ ⁻	2-	Boralkite
II-IV	BeO ₂ ²⁻	GeO ₂	2-	BeGeO

As an example of the manner in which the molecular sieve framework can be used in nanocomposite synthesis, first consider one of the simplest polyhedral cages in zeolite chemistry, the truncated octahedron found in the sodalite structure (Figure 7). This is in fact, an inorganic isomer of a fully saturated C₆₀ Buckminsterfullerene cluster, although slightly larger because of the longer (~1.6 Å) Si,Al-O bonds. The "four dimensional" character of the chemistry arises from the fact that one can carry out framework substitution reactions within the two dimensional surface and make use of potentially different chemical reactivities and geometric topologies inside and outside the cage. The cage dielectric properties and dimensions can be varied by the framework substitution shown in Table 1.

The 6 ring windows of the sodalite cage are large enough to permit the reversible inclusion of ions and water. The five atom cluster (Figure 8) is common with compositions such as (B₂O₄)₃ • Zn₄S [55], (B₂O₄)₃ • Zn₃GaP, and (BeSiO₄) • Cd₄Se [56]. In the sodalite type structures the cage has the same acentric point group

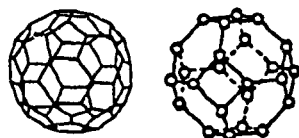


Figure 7. $[\text{Si}_2\text{Al}_{12}\text{O}_{36}]$ sodalite and C_{60} sixty atom polyhedra

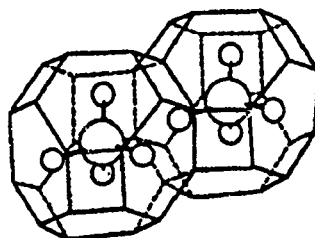


Figure 8. Sodalites with M_4X Clusters directly coupled through 6 rings

... ZnS or GaP , i.e. 43m, and contains (for example) the tetrahedral Zn_4S fragment which is the first coordination sphere of the sulfur atom in the bulk ZnS structure. One therefore has an expanded superlattice of Zn_4S molecular clusters (Figure 9). If one uses a larger anion, Se or Te, at the center of the sodalite cage, the Zn atoms are forced more towards the ultimate limit of being positioned at the center of the six ring openings. At that point the system becomes an expanded semiconductor lattice with all Zn atoms

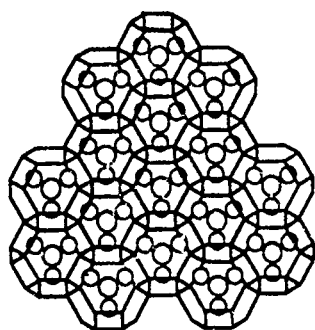


Figure 9. Zn_4X Sodalite Lattice

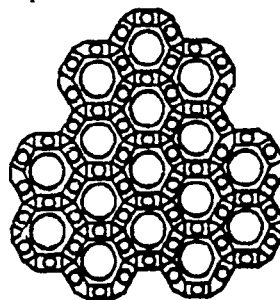


Figure 10. Expanded Semiconductor Lattice with Metal Atoms in Center of the Six Rings

equally spaced from all X atoms at the centers of the cages (Figure 10). In the structure of $(\text{B}_2\text{O}_4)_3 \cdot \text{Zn}_4\text{S}$ a 1.05 Å displacement of the zinc atoms is required to remove the Zn_4S cluster identity. Some Zn-S and cage to cage distances are given below (Table 2) to show how both cluster and intercluster geometry can be varied by the open framework surface. D is the metal atom displacement required for loss of cluster identity.

Table 2

Lattice (Å)	M-X Intercage (Å)	D(Å)	
$\text{Zn}_4\text{S B}$	2.260(3)	6.61	1.05
$\text{Zn}_4\text{S H}$	2.346(2)	7.03	1.17
$\text{Zn}_4\text{S HG}$	2.345(3)	7.16	1.24
$\text{Zn}_4\text{Se B}$	2.370(3)	6.66	0.96

B = Borallite = B_5O_{12}

H = Helvite = $\text{Be}_3\text{Si}_3\text{O}_{12}$

HG = GeHelvite = $\text{Be}_3\text{Ge}_3\text{O}_{12}$

The Zn-S distance in bulk is 2.34 Å, and in ZnSe the distance is 2.45 Å. In these structures intercluster coupling should be large and the band edges for the sulfide and selenide borallites are within 20 nm (blue shifted) of the bulk edge. The emission spectra at room temperature are intense and well defined with

corresponding excitation spectra which show considerable structure, and a sharp excitation peak at the absorption edge. In the case of $(\text{BeSiO}_4)_2 \cdot \text{Cd}_4\text{S}$ an emission excitation peak is also observed at the band edge.

The Ag_nX ($\text{X} = \text{group VII atom}$) clusters which make up the superlattice of the $[\text{Si}_6\text{Al}_6\text{O}_{24}]$ sodalite framework structure show remarkable structural and spectroscopic transformations as one varies the sodalite cage occupancy (57,58,59,60). At very low loadings the AgBr is a molecular silver halide unit with a AgBr internuclear distance (2.23(5) Å for AgBr in the $\text{Na}_{17}\text{Ag}_3$ cluster) which is shorter than that reported for gas phase silver bromide (2.39 Å). Due to more extensive covalent bonding of AgBr compared to NaBr the Na_3AgBr aggregate behaves like a slightly perturbed AgBr molecule with nearby Na^+ ions. In the fully exchanged Ag_4Br sodalites, the Ag-X ($\text{X} = \text{Cl}, \text{Br}, \text{I}$) distances are ~8% shorter than in the rock salt bulk materials. The intercage Ag-Ag distances are 25% to 12% longer (Cl^- to I^-) than in the bulk structure. Adjacent cages can be statistically emptied and the absorption lines followed from the a very sharp single line for the Ag-Br fragment at low loadings (similar to the gas phase values of 230 and 320 nm for the AgBr monomer) to the $\text{Ag}_4\text{Br}^{3+}$ isolated cluster to the fully loaded and intercage coupled system. The optical absorption data confirms the increased tunneling efficiency and intercage coupling as the distances between centers of the b cages decrease in the I^- to Cl^- sequence. Another interesting feature is evidence of a percolation threshold is seen in an abrupt change in the unit cell parameters and FT-far IR cation transitory modes as a function of loading.

Theoretical modelling of the potential well and intercluster coupling in the sodalite structure by ab initio calculations are currently in progress at Santa Barbara in collaboration with Horu Metiu. If the sodalite structure is synthesized with Na_4O^{2+} , NaOH can be Soxhlet extracted to give "empty" cages containing Na^{3+} . Gradual filling of these cages with sodium vapor at elevated temperatures gives a gradual change in colors from pink to dark blue. The chemical stability imparted by the inorganic framework is remarkable and the sodium metal loaded sodalite can be heated in water with no detectable reaction. The results clearly demonstrate the very strong dependence of absorption bands on the framework electric field and the sensitivity of the energy levels to small displacements of the sodium ions.

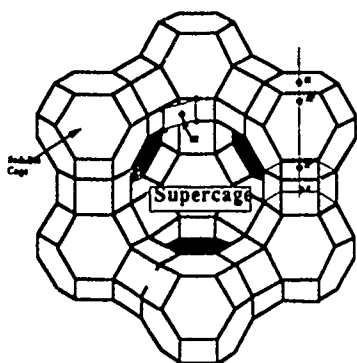


Figure 11. Structure and Ion exchange positions of cations for the Zeolite X structure. The 12-ring opening into the supercage is about 9 Å, and the supercage itself is 13 Å in diameter.

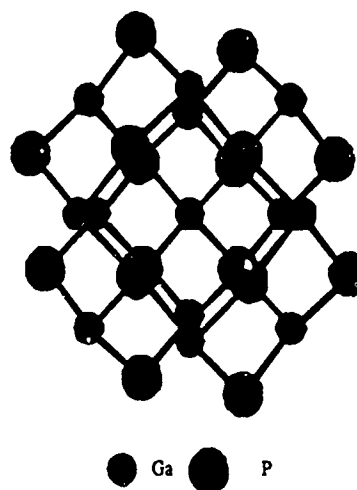


Figure 12. $\text{Ga}_{16}\text{P}_{13}$ Cluster based on EXAFS and MASNMR data

The sodalite cages can be interconnected in several ways to give different cage structures, e.g. Zeolite X has two types of cages available for cluster formation, the smaller 7 Å sodalite units and the larger 13 Å alpha cages (Figure 11). There are 5 sites (I, I', II, II', III) which are available for cation siting within the sodalite and

supercages. II-VI and I-VII quantum confined clusters can be synthesized by well understood ion-exchange methods, followed in the II-VI case by treatment with H_2S or H_2Se . It is important to note that the ion exchange process can yield very different siting of cations depending on temperature, pH, solvent vs. melt ion inclusion, other extra-framework ions, calcination, and loading levels. This process must be systematically controlled along with the conditions for treatment with H_2S or H_2Se in order to obtain materials which can be consistently reproduced and which contain monosize clusters. The ion exchange based inclusion chemistry of II-VI^[61,62,63,64,65] clusters have been investigated concentrating on the structural, optical, and photochemical^[66,67] aspects of the clusters.

Structural studies have been carried out using powder Rietveld X-ray diffraction methods^[68] which have established cubane like clusters of $(CdS)_4$ located in the sodalite cages of the structure. Extended X-ray absorption fine structure (EXAFS) spectroscopy was used to study the coordination sphere of Cd in the structure and showed that some of sulfur atom sites are occupied by oxygen atoms. These small cubes do not take advantage of the much larger area available to them in the supercages in this structure, and it is this intimate connection with the zeolite framework which probably makes this structure so stable.

Elemental and binary semiconductor synthesis by gaseous and melt diffusion within the zeolite host is being explored by a number of research groups, including Bogomolov^[69,70,71,72] (elemental semiconductors), Herron, Wang et al^[73] (Se), Endo^[74,75] (Se and Te), Goto^[76] (Te and Pb_2) and Ozin^[77,78,79] (MoO_3 and WO_3). Ozin and Goto have used careful concentration studies with different extraframework cations in different zeolite hosts to successfully demonstrate the fine tuning of optical and cluster structure which can be achieved with binary cluster synthesis and inclusion.

The advantages of using gas phase diffusion methods for inclusion can be illustrated by the synthesis of GaP in zeolite Y^[80]. Attempts to use ion exchange as a route to the formation of III-V semiconductors in zeolite frameworks resulted in the loss of crystallinity of the material due to the very low pH required to keep group III cations in solution as hydrated cations. Alternate methods of anhydrous nitrate and halide melts also failed to give the desired inclusion products, as did methylene chloride solutions of group III halides as precursors. The approach which succeeded in synthesizing GaP inside the pore structure of zeolite Y involves a metal organic chemical vapor deposition (MOCVD) approach. The reaction of $(CH_3)_3Ga$ with PH_3 is carried out within the pores of zeolites Na and HY at a series of temperatures to give small GaP particles which showed blue shifts in the UV-Vis spectra and upfield shifts in the solid state NMR; both indicative of size quantization effects. Extended X-ray absorption fine structure (EXAFS) spectroscopy identified particles which were $\sim 11 \text{ \AA}$ in diameter corresponding to 3 coordination spheres of the bulk structure, as illustrated in Figure 12.

This figure shows a possible cluster arrangement with either a Ga atom or P atom at the center of the cluster. In the case of a P atom at the center, the charge on the cluster must be balanced by connection to the anionic framework or residual methyl groups, but with a Ga atom at the center the charge could be accounted for by excess protons remaining on the P atoms due to incomplete phosphine dissociation. Synchrotron X-ray diffraction studies showed long range ordering of the clusters in the supercage, but a high degree of local disorder within the supercage. This observation supports the EXAFS data for clusters of about the size of the diameter of the supercage. Both EXAFS and solid state NMR support the model with a Ga atom at the center of the cluster. The primary concern with all zeolite inclusion materials is the ability to control diffusion properties so that the cluster distribution is homogeneous throughout the lattice. Even more so than for MOCVD deposition on 2-d substrates, diffusion kinetics must be defined and controlled. This will be the primary challenge to chemists for the synthesis of all 3-d quantum confined frameworks, regardless of the synthesis approach which is used.

The existence of polar molecular sieve structures provides access to an additional degree of control of cluster orientation. In this regard one dimensional polar pore structures are particularly promising for the alignment processes required for SHG. A non-centrosymmetric host could cause nanoclusters to dipole align, i.e. sulfides at one end and zincs at the other as is normally the case for ZnS, rather than a random polar orientation. This could be of some importance in magneto-optic materials. Non-centrosymmetric molecular sieves include ALPO-5^[81] (space group P6cc), ALPO-11^[82] (Ic2m), VPI-5^[83] (P6₃cm), sodalite^[84] (P4₃n) and offretite^[85] (P6m2). Variation in host framework charge density or dielectric constant, via Si/Al ratio changes, or the use of other framework atoms^[86], can be used to define the relative amounts of guest-host and guest-guest electrostatic interactions. For example, guest dipole molecules interact more strongly with one another in a low charge density host than in a high charge density host where guest-host interactions dominate. In a few charge density hosts, guest aggregation or chain formation should occur and lead to bulk dipole alignment. The counter ions present in the host can also be used to control guest aggregation. Changing the size of the ions alters the pore size and shape and the local electrostatic fields around the ions.

Conclusion:

The understanding and new synthetic approaches to nanocluster synthesis have opened extensive new vistas for all areas of science. The incorporation of nanoclusters into composite synthesis will require the continued development of highly sophisticated new chemical techniques and molecular engineering. Much will depend on the ability to utilize and understand the exterior surface chemistry of the nanophases. The health of the field has been demonstrated by rapid progress in optoelectronics and the recent isolation of large new polyhedral aromatic clusters. The chemistry of the latter introduces a "4th" dimension to nanocluster design. Similar considerations can be used to control cluster geometry and size distribution by the topography of three dimensional host surfaces, making it possible to create semiconductor quantum superlattices. The use of large three dimensional surface areas permits concentration studies of cluster interactions over a wide range, and at relatively high optical densities. It is to be expected that normally very unstable, nanosized phases can be synthesized and stabilized via encapsulation and integration with the open polyhedral framework systems that are now being developed.

Acknowledgements: The author wishes to particularly thank Louis Feron, Ying Wang, Karin Moller, Thomas Bein and Geoff Ozin for their help and many enlightening discussions. Research support of the Office of Naval Research, the National Science Foundation and E. I. du Pont is gratefully acknowledged.

REFERENCES:

1. L.E. Brus, *Proceedings of the 1st A. Welch Foundation Conference on Chemical Research*, XXXII Valency, 1988, pp. 4-67.
2. M.L. Steigerwald, L.E. Brus, *Ann. Rev. Mater. Sci.*, **19**, 471 (1989).
3. A. Henglein, *Top. Curr. Chem.*, **143**, 113 (1988).
4. S. Schmitt-Link, D.S. Chemla, and D.A.B. Miller, *Adv. Phys.*, **38**, 89 (1989).
5. D.A.B. Miller, *Optics & Photonics*, Feb. 7 (1990).
6. A. Cerotti, F. Longoni, I.L. Manassero, M. Manassero, G. Piva and M. Sansoni, *Angew. Chem. Int. Ed. Engl.*, **24**, 697 (1985).
7. D.M. Washochek, Ph.D. thesis, University of Wisconsin-Madison, 1980.
8. D.M. Washochek, E. J. Wucherer, L. F. Dahl, A. Ceriotti, G. Longoni, M. Manassero, M. Sansoni and P. Chini, *J. Am. Chem. Soc.*, **101**, 6110 (1979).
9. G. Schmid, *Polyhedron*, **7**, 2321-2329 (1988).
10. I.G. Dance, A. Chao, M.L. Scudder, *J. Am. Chem. Soc.*, **106**, 6285 (1984).
11. R. M. Herath-Banda, I.G. Dance, T. D. Bailey, D.C. Craig, M. L. Scudder *Inorg. Chem.*, **28**, 1862 (1989).
12. G.S.H. Lee, K. J. Fisher, D.C. Craig, M.L. Scudder, and I.G. Dance *J. Am. Chem. Soc.*, **112**, 6434 (1990).
13. G.S.H. Lee, D. C. Craig, I. Ma, M. L. Scudder, T. D. Bailey, and I. G. Dance, *J. Am. Chem. Soc.*, **110**, 4863 (1988).
14. L.T. Cheng, N. Heron, Y. Wang, *J. Appl. Phys.*, **66** (7), 3417 (1989).
15. L.E. Brus, *J. Phys. Chem.*, **90**, 2555 (1986).

16. M.L. Steigerwald, A.P. Alivisatos, J.M. Gibson, T.D. Harris, R. Kortan, A.G. Muller, A.M. Thayer, T.M. Duncan, and D. Douglas, *J. Am. Chem. Soc.* **110**, 3046 (1988).
17. N. Herron, Y. Wang, H. Eckert, *J. Am. Chem. Soc.* **112**, 1322 (1990).
18. M.N. Vargartik, V.P. Zagorodnikov, I.P. Stoyarov, I.I. Moiseev, V.A. I'ikholobov, et al., *J. Chem. Soc. Chem. Comm.* **1985**, p. 937.
19. G. Schmid, U. Giebel, W. Huster, A. Schwenk, *Inorg. Chim. Acta.* **85**, 97 (1984).
20. B.K. Teo, M.C. Hong, H. Zhang, D.B. Huang, *Angew. Chem. Int. Ed. Engl.* **26**, 897 (1987).
21. A. Fojtik, H. Weller, U. Koch, A. Henglein, *Ber. Bunsenges. Phys. Chem.* **88**, 969 (1984).
22. E.K. Byrne, L. Parkanyi, K. Theopold, *Science* **241**, 332 (1988).
23. P. Alivisatos and R. Wells, private communication.
24. W. Mahler, *Inorg. Chem.* **27**, 435 (1988).
25. T. Rajh, M.I. Vucemilovic, N.M. Dimitrijevic, O.I. Micic, A.J. Nozik, *Chem. Phys. Lett.* **143**, 305 (1988).
26. C.T. Dameron, R.N. Reese, R.K. Mehra, A.R. Kortan, P.J. Carroll, M.L. Steigerwald, L.E. Brus, D.R. Winge, *Nature* **338**, 596 (1989).
27. E. C. Thiel, *ACS Symp. Ser.* **372**, 179 (1988).
28. E. C. Thiel, *Annu. Rev. Biochem.* **56**, 289 (1987).
29. S. J. Lippard, *Angew. Chem. Int. Ed. Engl.* **27**, 344 (1988).
30. S.J. Lippard et al., *J. Am. Chem. Soc.* **109**, 3337 (1987).
31. S.C. O'Brien, Y. Liu, Q. Zhang, J.R. Heath, F.K. Tittel, R.F. Curl, R.E. Smalley, *J. Chem. Phys.* **84**, 4074 (1986).
32. K.D. Kolenbrander, M.L. Mandich, *J. Chem. Phys.* **90**, 5884 (1989).
33. Q. Zhang, W. Liu, R.F. Curl, F.K. Tittel, R.E. Smalley, *AIP Conference Proceedings*, **172**, (1987); *Adv. Laser Sci.-3* (1988).
34. J.M. Alford and R.E. Smalley, *Mater. Res. Soc. Symp. Proc.* **131**, Chemical Perspectives (1989).
35. Ph. Gerhardt, S. Löffler, and K. H. Homann, *Chem. Phys. Lett.* **137**, 306 (1987).
36. W. Kratschmer, L. D. Lamb, K. Iostropoulos, and D. R. Huffman, *Nature* **347**, xxx, (1990).
37. T. Ishihara, J. Takahashi, and T. Goto, *Solid St. Commun.* **69**, 933 (1989).
38. Y. Horikoshi, M. Kawashima, H. Yamaguchi, *Jpn. J. Appl. Phys.* **25**, L868 (1986).
39. Taken from M.A. Reed, R.T. Bate, K. Bradshaw, W.M. Duncan, W.R. Frensley, J.W. Lee, H.D. Shih, *J. Vac. Sci. Technol.* **B4**, 358 (1986).
40. R.D. Dupuis, R.C. Miller, P.M. Petroff, *J. Crystal Growth*, **68** (1), 398 (1984).

41. R.C. Miller, A.C. Gossard, D.A. Kleinman, O. Munteanu, *Phys. Rev.* **B29**, 7085 (1984).
42. P.M. Petroff, A.C. Gossard, R.A. Logan, W. Wiegmann, *Appl. Phys. Lett.* **41** (7), 635 (1982).
43. J. Cibert, P.M. Petroff, G.J. Dolan, S.J. Pearton, A.C. Gossard, J.H. English, *Appl. Phys. Lett.* **49**, 1275 (1986).
44. M.A. McCord, R.F.W. Pease, *J. Vac. Sci. Technol.* **B5**, 437 (1987).
45. C.J. Sandroff, J.P. Harbison, R. Ramesh, M.J. Andrejco, M.S. Hodge, D.M. Hwang, C.C. Chang, E.M. Vogel, *Science* **245**, 391 (1989).
46. G. Ozin, A. Stein, A. Kuperman, *Angew. Chem.* **101**, 373 (1989).
47. G.D. Stucky, J.E. MacDougall, *Science* (Washington, D. C., 1883-) **247**(4943), 669-78 (1990)
48. For good general references on zeolite Y and inolecular sieves in general, see D. W. Breck, "Zeolite Molecular Sieves" Robert E. Krieger, Publishing Co., Malabar, Fl (1984); R.M. Barrer, FRS, "Zeolites and Clay Minerals as Sorbents and Molecular Sieves", Academic Press, New York (1978).
49. M. E. Davis, C. Saldarriaga, C. Montes, J. Garces and C. Crowder, *Nature* **331**, 698 (1988); M. E. Davis, C. Saldarriaga, C. Montes, J. Garces and C. Crowder, *Zeolites* **8**, 362 (1988).
50. J. V. Smith and W.J. Dytrych, *Nature*, **309**, 607 (1984).
51. T. C. Sollner, P. E. Tannenwald, D. D. Peck, and W. D. Goodhue, *Appl. Phys. Lett.* **45**, 1319 (1984).
52. D. F. Nelson, R. C. Miller, D. A. Kleinman, and A. C. Gossard, *Phys. Rev. B* **34**, 8671 (1986).
53. B. F. Levine, K. K. Choi, C. G. Bethea, J. Walker, and R. J. Malik, *Appl. Phys. Lett.* **51**, 934 (1987).
54. L. C. West, and S. J. Eglash, *Appl. Phys. Lett.* **46**, 1156 (1985).
55. C. Fouassier, A. Levasseur, J. C. Joubert, J. Muller, P. Hagenmuller, *Z. Anorg. Allg. Chem.* **375** (2), 202 (1970).
56. K.L. Moran, W.T.A. Harrison, T.E. Gier, J.E. MacDougall, G.D. Stucky, *Mater. Res. Soc. Symp. Proc.*, **164**(Mater. Issues Microcryst. Semicond.), 123-8, (1990) and unpublished results.
57. A. Stein, P. M. Macdonald, G. A. Ozin, and G. D. Stucky, *J. Phys. Chem.* **94** (18), 6943 (1990).
58. G. A. Ozin, A. Stein, J. P. Godber and G. D. Stucky, *Proc. of the 5th International Symposium on Inclusion Phenomena and Molecular Recognition*, J Atwood, ed, 379 (1990).
59. A. Stein, G.A. Ozin, G.D.Stucky, *J. Am. Chem. Soc.* **112**, 904 (1990).
60. A. Stein, G.A. Olzin and G.D. Stucky, *J. soc. Photogr. Sci. Technol. Japan*, **53**, 001 (1990).
61. Y. Wang, N. Herron, *J. Phys. Chem.* **91**, (2), 257 (1987).
62. Y. Wang, N. Herron, *J. Phys. Chem.* **92** (17), 4988 (1988).
63. N. Herron, Y. Wang, M.M. Eddy, G.L. Stucky, D.E. Cox, K. Moller, T. Bein, *J. Am. Chem. Soc.* **111** (2), 530 (1989).

64. K. Moller, M.M. Eddy, G.D. Stucky, N. Herron, T. Bein, *J. Am. Chem. Soc.* **111** (7), 2564 (1989).
65. X.Liu and J.K. Thomas, *Langmuir* **5** (1), 58 (1989).
66. R.D. Stramel, T. Nakamura, J.K. Thomas, *J. Chem. Soc., Faraday Trans. 1* **84** (5), 1287 (1988).
67. M.A. Fox, T.L. Pettit, *Langmuir* **5** (4), 1056 (1989).
68. N. Herron, Y. Wang, M.M. Eddy, G.D. Stucky, D.E. Cox, K. Moller, T. Bein, *J. Am. Chem. Soc.* **111**, 530 (1989).
69. V. N. Bogomolov, E. L. Lutsenko, V. P. Petranovskii, S. V. Kholodkevich, *Pis'ma Zh. Eksp. Teor. Fiz.* **23**(9), 528-30 (1976).
70. V. N. Bogomolov, V. V. Poborchii, S. V. Kholodkevich, *Pis'ma Zh. Eksp. Teor. Fiz.* **31**(8), 464-7 (1980).
71. V. N. Bogomolov, A. I. Zadorozhnyi, V. P. Petranovskii, A. V. Fokin, S. V. Kholodkevich, *Pis'ma Zh. Eksp. Teor. Fiz.* **29**(7), 411-14 (1979).
72. V.N. Bogomolov, I.B. Vendik, V.V. Esipov, V.V. Zadorozhnyi, T.M. Pavlova, *Radiotekh. Elektron. (Moscow)* **32**(9), 2000-2 (1987).
73. J. B. Parise, J. E. Mac Dougall, N. Herron, R. Farlee, A. W. Sleight, Y. Wang, T. Bein, K. Moller, L. M. Moroney, *Inorg. Chem.* **27**(2), 221-8 (1988).
74. H. Endo, M. Yao, Hyomen **25**(6), 394-9 (1987).
75. Y. Katayama, M. Yao, Y. Ajiro, M. Inui, H. Endo, *J. Phys. Soc. Jpn.* **58**(5), 1811-22 (1989).
76. Y. Nozue, Z.K. Tang and T. Goto, *Solid State Comm.* **73**, 531 (1990).
77. S. Ozkar, G.A. Ozin, K. Moller, T. Bein, *J. Am. Chem. Soc.* **112**(26), 9575-86 (1990).
78. G.A. Ozin, S. Ozkar, *J. Phys. Chem.* **94**(12), 7556-62 (1990).
79. G.A. Ozin, S. Ozkar, P. Macdonald, *J. Phys. Chem.* **94**(18), 6939-43 (1990).
80. J.E. Mac Dougall, H. Eckert, G.D. Stucky, N. Herron, Y. Wang, K. Moller, T. Bein, D. Cox, *J. Am. Chem. Soc.*, **111**, 8006 (1989).
81. Bennet, J.M.; Cohen, J.P.; Flanigen, E.M.; Pluth, J.J.; Smith, J.V. in: *Intrazeolite Chemistry, ACS Symposium Series 218*, eds. G.D. Stucky and F.G. Dwyer, American Chemical Society: Washington, D.C., 1983, p. 109-118.
82. J.M. Bennett, J.W. Richardson, Jr., J.J. Pluth, J.V. Smith, *Zeolites*, **6**, 160 (1987).
83. M.E. Davis, C. Saldaña, C. Montes, J. Garces, C. Crowder, *Nature* **331**, 698(1988); *Zeolites* **8**, 362 (1988).
84. J. Felsche, S. Luger, Ch. Baerlocher, *Zeolites* **6**, 367 (1986).
85. J.A. Gard, J.M. Tait, *Acta. Cryst.* **B28**, 825 (1972).
86. R.L. Bedard, S.T. Wilson, L.D. Vail, J.M. Bennet, E.M. Flanigen, "Zeolites: Facts, Figures, Future", *Studies in Surface Science and Catalysis*, **49**, (1989), P. A. Jacobs and R. A. van Santen, Eds. 375-387.

TECHNICAL REPORT DISTRIBUTION LIST - GENERAL

Office of Naval Research (2)*
Chemistry Division, Code 1113
800 North Quincy Street
Arlington, Virginia 22217-5000

Dr. James S. Murday (1)
Chemistry Division, Code 6100
Naval Research Laboratory
Washington, D.C. 20375-5000

Dr. Robert Green, Director (1)
Chemistry Division, Code 385
Naval Air Weapons Center
Weapons Division
China Lake, CA 93555-6001

Dr. Elek Lindner (1)
Naval Command, Control and Ocean
Surveillance Center
RDT&E Division
San Diego, CA 92152-5000

Dr. Bernard E. Douda (1)
Crane Division
Naval Surface Warfare Center
Crane, Indiana 47522-5000

Dr. Richard W. Drisko (1)
Naval Civil Engineering
Laboratory
Code L52
Port Hueneme, CA 93043

Dr. Harold H. Singerman (1)
Naval Surface Warfare Center
Carderock Division Detachment
Annapolis, MD 21402-1198

Dr. Eugene C. Fischer (1)
Code 2840
Naval Surface Warfare Center
Carderock Division Detachment
Annapolis, MD 21402-1198

Defense Technical Information
Center (2)
Building 5, Cameron Station
Alexandria, VA 22314

* Number of copies to forward